

THE KINEMATICS OF THE PLANETARY NEBULAE IN THE LARGE MAGELLANIC CLOUD

STEPHEN J. MEATHERINGHAM AND MICHAEL A. DOPITA

Mount Stromlo and Siding Spring Observatories, Australian National Observatory

HOLLAND C. FORD

Space Telescope Science Institute, Johns Hopkins University

AND

B. LOUISE WEBSTER

School of Physics, University of New South Wales

Received 1987 January 28; accepted 1987 October 13

ABSTRACT

The radial velocities of a total of 94 planetary nebulae (PN) in the Large Magellanic Cloud (LMC) have been determined. This kinematics of the population of planetary nebulae is compared with the H I data in the context of a reanalysis of the survey by Rohlfs *et al.*, taking into account the transverse velocity of the LMC. We find that the best solution for this transverse velocity is $275 \pm 65 \text{ km s}^{-1}$ and that the LMC is near perigalacticon. This is consistent with a maximum Galactic mass of order $4.5 \times 10^{11} M_{\odot}$ out to 51 kpc. The rotation curve obtained after correction for this velocity implies a mass of $(4.6 \pm 0.3) \times 10^9 M_{\odot}$ within a radius of 3° , or about $6 \times 10^9 M_{\odot}$, total. The rotation solution for the PN population is essentially identical with that of the H I but the vertical velocity dispersion of 19.1 km s^{-1} is much greater than the value of 5.4 km s^{-1} found for the H I. This increase in velocity dispersion is consistent with it being the result of orbital heating and diffusion operating in the LMC in a manner essentially identical with that found for the solar neighborhood.

Subject headings: galaxies: internal motions — galaxies: Magellanic Clouds — nebulae: planetary — radio sources: 21 cm radiation

I. INTRODUCTION

The Magellanic Clouds hold the solution to many of the unanswered questions about planetary nebulae (PN) by furnishing us with a large luminosity-limited sample at a common and known sample, with low reddening, and close enough that it can be observed in detail. Previous papers in our studies of the Magellanic Cloud PN have tended to concentrate on evolutionary problems of the PN themselves (Dopita *et al.* 1985; Dopita, Ford, and Webster 1985; Dopita *et al.* 1987, 1988; Meatheringham, Dopita, and Morgan 1988; Wood, Dopita, and Bessel 1985; Wood *et al.* 1987).

Both the SMC and the LMC are of considerable interest from a kinematical viewpoint. The tidal interaction of the Clouds with each other and with the Galaxy appears to have been quite significant in recent times (Murai and Fujimoto 1980). The SMC in particular appears to have been considerably disrupted by a recent close passage to the LMC (Mathewson and Ford 1984; Mathewson 1984; Mathewson, Ford, and Visvanathan 1986). Our survey of the kinematics of the PN in the SMC suggests that the stellar component has certainly been randomized, but that gaseous tidal arms project from the stellar core of the SMC (Dopita *et al.* 1985). For the LMC, Freeman, Illingworth, and Oemler (1983) report the enigmatic finding that the young and old populations have significantly different rotation solutions. The old population of clusters has its line of nodes rotated by some 49° with respect to the younger clusters with ages less than 10^9 yr. The data on the planetary nebulae were sparse but appeared to be in agreement with the "young" solution.

The PN form a population with an age intermediate between the H I and young clusters and the old Population II clusters, and therefore a detailed study of their kinematics

might be expected to cast new light on this problem. Previous to the results reported in this paper, there have been only three kinematic studies of the LMC PN, which together furnish radial velocities for some 35 objects. In this paper we present new kinematical data for a total of 95 objects. By combining these data with a reanalysis of the H I survey of Rohlfs *et al.* (1984), we have been able to estimate the transverse velocity of the LMC, generate a new rotation curve and mass estimate for the LMC, and derive a typical age and precursor mass for the population of PN in the LMC.

II. OBSERVATIONS AND DATA REDUCTION

a) Selection of Objects

The majority of the objects we have observed appear in the list of Sanduleak, McConnell, and Philip (SMP) (1978) which gives 103 PN in the LMC and 28 in the SMC. Many of these were previously known to be emission nebulae (Henize 1956; Lindsay and Mullen 1963), and a fair number had been positively identified as PN by Henize and Westerlund (1963). Throughout this paper we have identified objects by their SMP number, this being the most comprehensive and unambiguous listing to date. The Jacoby (J) (1980) objects present a more difficult group. Many of these are faint and could not be definitely confirmed as PN even with the AAT 3.9 m telescope at the dispersion we were using. Only five objects gave data of sufficiently high quality to be included here. Recently Morgan and Good (1985) undertook a search for LMC planetary nebulae using an objective prism on the UK Schmidt telescope at Siding Spring. We observed, and confirmed, a total of seven new candidates in the northern part of the LMC in a list of 31.

The spatial distribution of the observed PN is shown in Figure 1, along with outer H I contours from Mathewson and

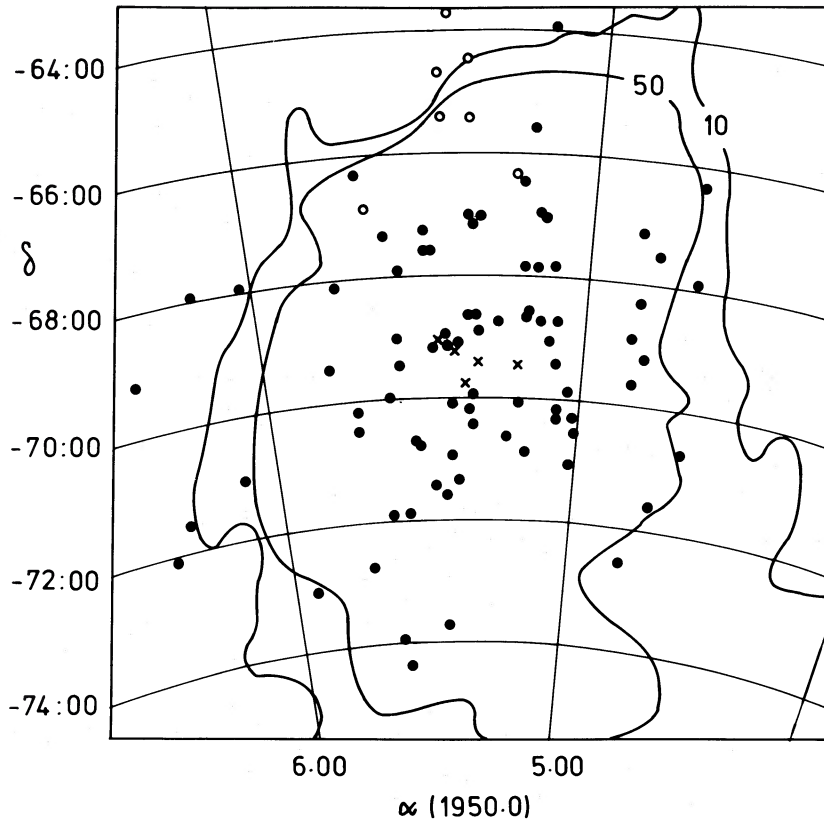


FIG. 1.—The spatial distribution of the LMC planetaries. Filled circles represent the SMP (1978) objects, open circles the Morgan (1984) objects, and crosses the Jacoby (1980) nebulae. Outer H I contours from Mathewson and Ford (1984) are also shown (units of atoms cm^{-2} in line of sight).

Ford (1984). There is little difference between the spatial locations of the PN and the H I in this diagram.

b) The Observations and Results

We have used three telescopes, two spectrographs, and two photon-counting systems in this study. Observations in 1983 October and November and 1984 October were with the 1.0 m telescope at Siding Spring Observatory, and observations in 1985 January used the 2.3 m Advanced Technology Telescope at Siding Spring. Both of these telescopes are operated by the Australian National University. The spectrograph was a Perkin-Elmer échelle and the detector the photon-counting array (PCA) (Stapinski, Rodgers, and Ellis 1981). The faintest objects were observed in 1983 December using the 3.9 m Anglo-Australian Telescope (AAT) with its Royal Greenwich Observatory spectrograph and the image photon counting system (IPCS).

The instrumental parameters and the reduction procedures have already been described (Dopita *et al.* 1985) and will not be repeated here. The resolutions of both systems are very similar, 11.5 km s^{-1} FWHM for the échelle system, and 11.75 km s^{-1} FWHM for the AAT system. For objects with a high signal-to-noise ratio, and with relatively narrow line profiles, our estimated ultimate errors in the determination of radial velocities are $\pm 1.5 \text{ km s}^{-1}$ for the 1.0 m observations, $\pm 0.6 \text{ km s}^{-1}$ for the 2.3 m data, and $\pm 0.3 \text{ km s}^{-1}$ in the case of the AAT measurements (see also Dopita *et al.* 1985). For those objects with large expansion velocities, measurement errors are greater and can be estimated as $\pm \sigma/N^{1/2}$, where σ is the e -folding width of the Gaussian fit and N is the number of photons in the profile

(Bevington 1969). With this definition, we find that the maximum error could be as large as 4.8 km s^{-1} . This error can be checked for those objects for which repeated observations exist. In the following list, the difference between the individual determinations is given in units of km s^{-1} . Shown in parentheses is the error estimated in the manner given above. SMP 5, 0.03 (0.1); SMP 6 0.09 (0.2); SMP 11, 2.42 (1.8); SMP 21, 1.35 (1.4); SMP 23, 0.4 (0.7); SMP 47, 0.72 (0.9); SMP 94, 3.33 (3.0); J 26, 3.83 (2.7); J 33, 1.72 (1.9). The mean ratio of the observed velocity difference to the expected error is 0.87, compared with a figure of 0.95 expected for a Gaussian distribution of errors.

In Table 1 we present the measured radial velocities, corrected to local standard of rest (LSR), positions the telescopes used in the observations, and our estimated error for each object. The radial velocity given is the area weighted mean in the cases were more than one Gaussian component was needed to fit the profile. It might be argued that, in the case of those objects which show two separated components, the simple mean might have been a more accurate representation of the radial velocity. In these cases the radial velocity given by this procedure is shown in parentheses.

c) Comparison with Earlier Results

There have been three earlier studies of the kinematics of the LMC planetary nebulae; that of Feast (1968) (25 PN), of Webster (1969) (14 PN) and of Smith and Weedman (1972) (27 PN). There is substantial overlap of objects observed in these studies, which together yield radial velocities for a total of 35 objects. The earlier work was with low-dispersion spectro-

TABLE 1
RADIAL VELOCITY DATA FOR LMC PLANETARY NEBULAE

Object ^a	R.A. (1950.0)	Decl. (1950.0)	V_{LSR}	Telescope ^b	Object ^a	R.A. (1950.0)	Decl. (1950.0)	V_{LSR}	Telescope ^b
SMP 1	4 ^h 38 ^m 59 ^s .9	-70°42'32"	209.1 ± 0.2	b	SMP 57	5 24 01	-69 14 00	297.7 ± 1.1	a
SMP 2	4 41 00.4	-67 53 49	248.2 ± 0.2	b	SMP 58	5 24 36	-70 06 00	264.2 ± 0.3	a
SMP 3	4 42 12.8	-66 18 47	172.0 ± 0.2	b	SMP 60	5 24 53.7	-70 56 34	207.0 ± 4.8	a
SMP 4	4 43 57.6	-71 35 40	283.0 ± 1.1	b	SMP 61	5 25 48.8	-73 43 18	178.4 ± 0.9	a
SMP 5	4 48 08.3	-67 31 18	271.0 ± 0.1 (271.2)	a, b	SMP 62	5 25 40.6	-71 35 29	223.6 ± 0.5	a
SMP 6	4 48 27.7	-72 33 33	249.0 ± 0.2	a, b	SMP 63	5 25 44.3	-68 58 30	248.8 ± 0.4	a
SMP 7	4 48 43	-69 13 34	204.9 ± 1.9	a	SMP 65	5 28 13	-71 27 00	195.7 ± 0.9	a
SMP 8	4 50 31.3	-69 38 58	277.1 ± 0.8	a	SMP 66	5 28 49	-67 35 00	289.2 ± 1.1	a
SMP 9	4 50 35	-68 18 31	270.7 ± 1.1	a	SMP 67	5 29 22.7	-67 35 07	274.1 ± 0.9	a
SMP 10	4 51 20.6	-68 53 02	207.0 ± 1.4 (207.1)	a	SMP 69	5 29 24	-67 15 01	289.9 ± 2.9	a
SMP 11	4 51 35.8	-67 10 15	249.4 ± 1.8 (273.2)	a, c	SMP 71	5 30 48	-70 46 01	201.2 ± 0.5	a
SMP 13	5 00 34	-70 31 11	212.3 ± 1.5	a	SMP 73	5 31 36	-70 42 00	225.6 ± 0.4	a
SMP 14	5 00 54.5	-71 03 10	236.9 ± 2.6	c	SMP 74	5 33 54	-71 53 00	253.6 ± 1.1	a
SMP 15	5 01 19.4	-70 17 57	188.0 ± 1.2	a	SMP 76	5 34 06.1	-67 55 06	262.8 ± 0.9 (268.9)	a
SMP 16	5 02 24.8	-69 53 03	237.5 ± 1.5	a	SMP 77	5 34 29.8	-69 28 13	328.2 ± 0.3	a
SMP 18	5 04 13	-70 11 01	228.7 ± 1.4	a	SMP 78	5 34 39.6	-69 00 19	240.7 ± 1.1	a
SMP 19	5 04 16	-70 18 03	220.2 ± 0.8	a	SMP 79	5 34 55	-74 22 00	215.1 ± 0.8	a
SMP 20	5 04 59.3	-69 25 39	273.1 ± 1.7	a	SMP 81	5 36 07	-73 56 00	242.2 ± 1.1	a
SMP 21	5 05 05.1	-68 43 08	243.7 ± 1.4 (232.4)	a, c	SMP 82	5 36 26.5	-70 00 01	239.6 ± 0.9 (239.9)	c
SMP 23	5 06 15.0	-67 49 21	268.0 ± 0.7	a	SMP 83	5 36 25.8	-67 19 57	276.2 ± 0.5 (279.4)	a, b, c
SMP 24	5 06 34.0	-69 03 24	254.7 ± 3.5	c	SMP 84	5 37 13	-71 54 00	235.0 ± 0.2	a
SMP 27	5 08 00	-67 01 12	258.2 ± 2.2	a	SMP 85	5 40 29.7	-66 19 04	217.0 ± 0.3	a
SMP 28	5 08 11.9	-68 55 35	233.7 ± 2.4	c	SMP 87	5 42 06.6	-72 43 35	264.6 ± 1.0	a
SMP 29	5 08 17.4	-68 44 03	228.2 ± 0.8	a	SMP 88	5 43 08.5	-70 30 43	211.0 ± 2.0	a
SMP 30	5 09 18	-66 57 26	264.9 ± 1.0 (264.3)	a	SMP 89	5 43 07.5	-70 10 50	261.2 ± 0.6	a
SMP 31	5 09 26.4	-67 51 08	248.1 ± 0.4	a	SMP 91	5 45 12	-68 06 59	295.3 ± 1.5	b
SMP 32	5 10 11.7	-70 52 50	240.2 ± 1.7	a	SMP 92	5 47 27.8	-69 28 32	256.4 ± 0.7	a
SMP 33	5 10 26	-68 33 49	253.9 ± 1.0	a	SMP 94	5 55 15.9	-73 03 02	256.8 ± 3.0	a, b
SMP 35	5 10 45	-65 33 02	295.0 ± 1.0 (297.8)	a	SMP 95	6 01 57.3	-67 55 58	290.9 ± 0.9	b
SMP 36	5 10 51	-68 39 48	247.6 ± 2.6	a	SMP 96	6 06 46.7	-71 03 49	239.5 ± 2.0	a
SMP 37	5 11 14	-67 50 57	255.2 ± 1.5	a	SMP 97	6 10 36.5	-67 55 44	271.8 ± 0.6 (271.6)	b
SMP 38	5 11 51	-70 04 46	225.4 ± 0.9	a	SMP 99	6 19 45.9	-71 34 35	248.8 ± 0.3	b
SMP 40	5 12 11.7	-66 26 25	238.9 ± 1.9 (237.0)	a	SMP 100	6 24 08	-72 06 08	270.1 ± 0.8	b
SMP 41	5 13 59.1	-70 36 55	244.2 ± 1.9 (265.1)	a	SMP 101	6 23 52	-69 09 08	266.0 ± 1.0 (267.5)	b
SMP 42	5 16 02	-68 45 36	273.4 ± 1.7	a	SMP 102	6 29 41	-68 00 55	286.5 ± 1.2	b
SMP 45	5 19 22.2	-67 01 10	275.0 ± 1.0	a	J5	5 12 07.9	-69 27 13	262.9 ± 0.6	b
SMP 46	5 19 45.6	-68 54 07	258.0 ± 1.0	c	J26	5 20 22.6	-69 28 53	227.8 ± 2.7 (236.0)	a, b
SMP 47	5 20 17.8	-69 34 00	256.6 ± 0.9 (249.5)	a, b	J33	5 21 42.3	-69 45 51	231.9 ± 1.9	a, b
SMP 48	5 20 35.5	-69 56 34	240.8 ± 0.2	a	J38	5 24 55.7	-69 08 27	265.6 ± 1.2 (272.3)	b
SMP 49	5 20 30	-70 27 01	232.2 ± 1.2 (235.7)	a	J41	5 26 29.6	-60 03 28	240.0 ± 1.1 (239.9)	b
SMP 50	5 20 54.5	-67 08 37	284.1 ± 1.2	a	A0	5 25 46.0	-63 39 30	283.4 ± 0.5	a, b
SMP 51	5 21 22.0	-70 12 24	256.4 ± 0.5	a	A3	5 21 46.9	-64 28 03	272.9 ± 0.5	b
SMP 52	5 21 38.8	-68 38 27	256.9 ± 1.0	a	A4	5 26 30.8	-64 40 28	254.2 ± 2.0 (243.4)	a, b
SMP 53	5 21 37	-67 01 00	261.8 ± 0.7	a	A22	5 21 36.7	-65 25 16	236.7 ± 0.9	a, b
SMP 54	5 21 58.6	-68 42 10	265.4 ± 1.7 (278.1)	a, b	A24	5 26 10.8	-65 24 15	267.2 ± 1.3	b
SMP 55	5 23 22.8	-71 21 52	194.7 ± 0.3	a	A46	5 13 23.8	-66 20 52	243.4 ± 1.3 (259.1)	b
SMP 56	5 23 50.4	-69 06 45	276.1 ± 0.4	c	A54	5 39 17.3	-66 51 17	282.8 ± 1.9	b

NOTE.—Velocities in km s⁻¹.^a SMP = Sanduleak, McConnell, and Philip 1978; J = Jacoby 1980;

A = Morgan 1984.

^b a = 1 m; b = 2.3 m; c = 3.9 m.

TABLE 2
COMPARISON WITH RADIAL VELOCITIES OBTAINED IN EARLIER STUDIES

OBJECT	HELIOCENTRIC RADIAL VELOCITY (km s^{-1})						
	SMP	N	WS	This Study	Feast	Webster	Smith and Weedman
1.....	182	1	224.7	219	...	224	
6.....	184	2	264.6	271	...	263	
15.....	...	5	203.1	202	
19.....	188	6	235.2	239	...	236	
21.....	97	7	260.5	250	283	262	
23.....	24	8	282.4	302	301	281	
32.....	192	10	263.6	247	...	257	
38.....	110	15	240.5	243	...	238	
47.....	122	18	...	275	280	269	
48.....	123	19	255.7	...	258	...	
50.....	39	20	299.9	337	317	296	
52.....	124	21	272.7	280	...	270	
53.....	42	22	277.7	277	...	278	
58.....	133	23	279.4	276	
61.....	203	24	192.6	185	
62.....	...	25	238.3	...	250	238	
63.....	...	26	264.1	...	280	264	
66.....	52	27	304.9	308	
73.....	208	29	240.5	239	241	236	
74.....	209	30	268.2	262	
75.....	151	31	297	
76.....	...	32	278.2	...	295	280	
78.....	153	33	256.1	252	262	258	
79.....	210	...	229.3	230	
81.....	211	34	256.3	234	
83.....	66	35	288.2	287	296	...	
84.....	212	36	249.6	261	...	251	
87.....	215	37	279.6	284	
89.....	178	38	276.4	276	270	277	
92.....	170	39	271.7	274	...	271	
97.....	...	40	288.4	293	
98.....	...	41	...	262	
99.....	221	42	264.2	263	254	258	
Mean Difference (km s^{-1}) (Other study - this study)				+1.39	+8.54	-1.50	

raphs and photographic plates, but the Smith and Weedman study used a single-channel, photoelectric, pressure-scanned Fabry-Pérot interferometer with a resolution almost identical to ours (11 km s^{-1} , FWHM).

Table 2 compares our measurements with these three earlier determinations. The radial velocities are given in the heliocentric system. As was found in our kinematical study of the SMC (Dopita *et al.* 1985), there is excellent agreement with the Feast (1968) results, the mean difference being only 1.39 km s^{-1} for the 23 objects in common. The Webster (1969) data appear to have a systematic error, in the sense that radial velocities are overestimated by 8.5 km s^{-1} , for both the LMC and SMC. This is probably the result of the different conditions of illumination between the observations and the comparison lamp exposures. However, if this error is taken into account, the scatter is very similar to the Feast (1968) data. As might have been expected given the comparable resolutions, the agreement between our determinations and the Smith and Weedman (1972) measurements is excellent. The results differ by only 1.5 km s^{-1} in the mean, with an RMS scatter of only 3.0 km s^{-1} .

III. THE H I KINEMATICS OF THE LMC

a) H I Surveys

Since the H I surveys of the LMC give a detailed and global coverage, the H I data give a very useful (young) reference

frame with which to compare and contrast the kinematics of the older PN population. The first extensive H I survey of the LMC was by McGee and Milton (1964, 1966a, b), but this has been supplanted, at least in the central 6° or so, by the Rohlfs *et al.* (1984) work, hereafter RKSF. This gives H I velocities to a precision of $\pm 1 \text{ km s}^{-1}$ in a regular grid spacing of $\Delta\alpha \approx 2$ minutes, 20 s and $\Delta\delta = 12'$, over a total of 1023 points.

The derivation of both a reliable rotation curve and the orientation parameters from such data is not a straightforward task. First, the large angular diameter of the LMC and its large transverse velocity (of order 300 km s^{-1} ; Mathewson, Schwartz, and Murray 1977; Feitzinger, Isserstedt, and Schmidt-Kaler 1977; Lin and Lynden-Bell 1982) ensure that there will be a substantial velocity gradient in the direction of motion. This probably accounts for the rotation between the geometrical line of nodes of $168^\circ \pm 4^\circ$ (Feitzinger, Isserstedt, and Schmidt-Kaler 1977) and the kinematically determined value of 208° (RKSF). If the LMC is a rotating flat disk, the regular velocity gradient resulting from the transverse motion will be combined with the "spider" diagram of the rotation curve to both change the maximum velocity gradient and to twist the lines of constant velocity, particularly in the outer regions. This effect could, in some circumstances, simulate a warp in the H I disk.

A second problem is that the LMC is seen nearly face-on. The best estimates of its inclination are $31^\circ \pm 8^\circ$ derived from the luminosity gradient of the Cepheids (de Vaucouleurs 1960) and a value of $33^\circ \pm 3^\circ$ estimated from both the H I and optical distributions (Feitzinger, Isserstedt, and Schmidt-Kaler 1977). This ensures a relatively feeble projection of the rotation into radial velocities and allows local perturbations in the vertical velocity distribution to confuse and mask rotation. Such effects are known to occur in regions of active star formation such as 30 Dor or in LMC Constellation III (Caulet *et al.* 1982; Dopita, Mathewson, and Ford 1985).

The third complicating factor is the possibility of ram-pressure stripping of the outer H I envelope caused by the passage of the LMC through the tenuous hot outer corona of our Galaxy. This may be the most plausible explanation for the origin of the Magellanic Stream (Mathewson, Cleary, and Murray 1974; Mathewson, Schwartz, and Murray 1977). Circumstantial evidence to support this viewpoint may be found in the displacement of the globular cluster system to the NE (Freeman, Illingworth, and Oemler 1983), and the steep gradient in the H I column density in this sector of the LMC, in the presumed direction of motion (Mathewson, Cleary, and Murray 1974). The RKSF data also suggest that the gas in this portion of the LMC has been considerably disturbed. This sector of the LMC displays split line profiles. One component merges into the H I disk of the rest of the LMC, and we identify this as relatively undisturbed disk H I, which we have used in our further analysis of the disk kinematics. However, the other component, with higher radial velocity, appears to be a dynamically distinct entity and may represent either a grossly warped outer disk, or else a stream of ram-pressure stripped gas originating at the "leading" edge of the LMC.

b) The Transverse Velocity of the LMC

In principle, the magnitude of the transverse velocity of the LMC can be estimated from the transverse velocity gradient which it gives rise to across the face of the LMC provided that the orbital plane of the LMC is known. Previous workers (Mathewson, Cleary, and Murray 1974; Mathewson, Schwartz, and Murray 1977) have already noted that the Magellanic

stream holds the key to this problem. As seen from the Sun, the Magellanic stream defines a small circle in the sky. However, provided that the distance to the stream is of order 50 kpc, it will define a great circle as seen from the Galactic center, passing through the LMC at position angle $110^\circ \pm 10^\circ$.

Both the ram-pressure stripping models of the origin of the stream (Meurer, Bicknell, and Gingold 1985) and the tidal interaction models (Lin and Lynden-Bell 1982; Fujimoto and Murai 1984) predict that, provided that the tail of the stream is not too close, the stream will extend along the orbital plane of the Magellanic Clouds. This result is independent of whether the stream leads or lags the Magellanic Clouds. Thus we can take the orbital plane to be defined as the great circle the stream extends along as seen from the Galactic center.

In order to estimate the magnitude of the transverse velocity of the LMC in this plane, we have investigated the effect of the transverse velocity gradient on the direction of the kinematical line of nodes as defined in the central 2° of the LMC. The correct value of the transverse velocity is found when applying its inverse rotates the kinematical line of nodes to lie in the same direction as the photometric line of nodes. The effect of this correction is shown of Figure 2, which implies that the correct transverse velocity of the LMC is $275 \pm 65 \text{ km s}^{-1}$. The size of the error bar is defined principally by the uncertainty in the photometric line of nodes ($\pm 4^\circ$); the uncertainty in the kinematical line of nodes ($\pm 1^\circ$) is small but not negligible. Figure 3 shows the H I isovelocity contour plot resulting from the appli-

cation of this correction, adopting only the "disk" component of the H I in the region of split line profiles discussed above. This diagram bears a much closer resemblance to the classical "spider" diagram than do the "raw" H I data (RKSF). Perturbations in the isovelocity plot reflect regions of star formation such as 30 Dor, Constellation III, or other supergiant shells (Meaburn 1981). There also appears to be a perturbation associated with the bar of the LMC, which could be a result of the gas streaming motions expected on theoretical grounds (de Vaucouleurs and Freeman 1973).

c) The Orbit of the LMC and Mass of the Galaxy

The total orbital energy of the LMC with respect to the Galaxy can now be calculated, provided that the Galactocentric distance can be computed and that the effect of the solar motion can be taken out. The distance modulus of the LMC has been estimated from a variety of methods to be 18.5 ± 0.1 (Feast 1984; Visvanathan 1985). In galactic coordinates, therefore, the position vector from the Sun to the LMC, L , is $L = 50.1 \pm 2.3 (0.153, -0.826, -0.540)$ kpc. Here the distance with its error is given, and the direction cosines are given in parentheses. This figure can be compared with the value of 52 kpc adopted by Lin and Lynden-Bell (1982). The position vector of the Sun with respect to the Galactic center is $S = 8.7 \pm 1.0 (1, 0, 0)$ (see review by Graham 1979). Hence, the distance from the Galactic center to the LMC is $|L - S| = 51 \pm 3$ kpc. The geometry of the situation ensures

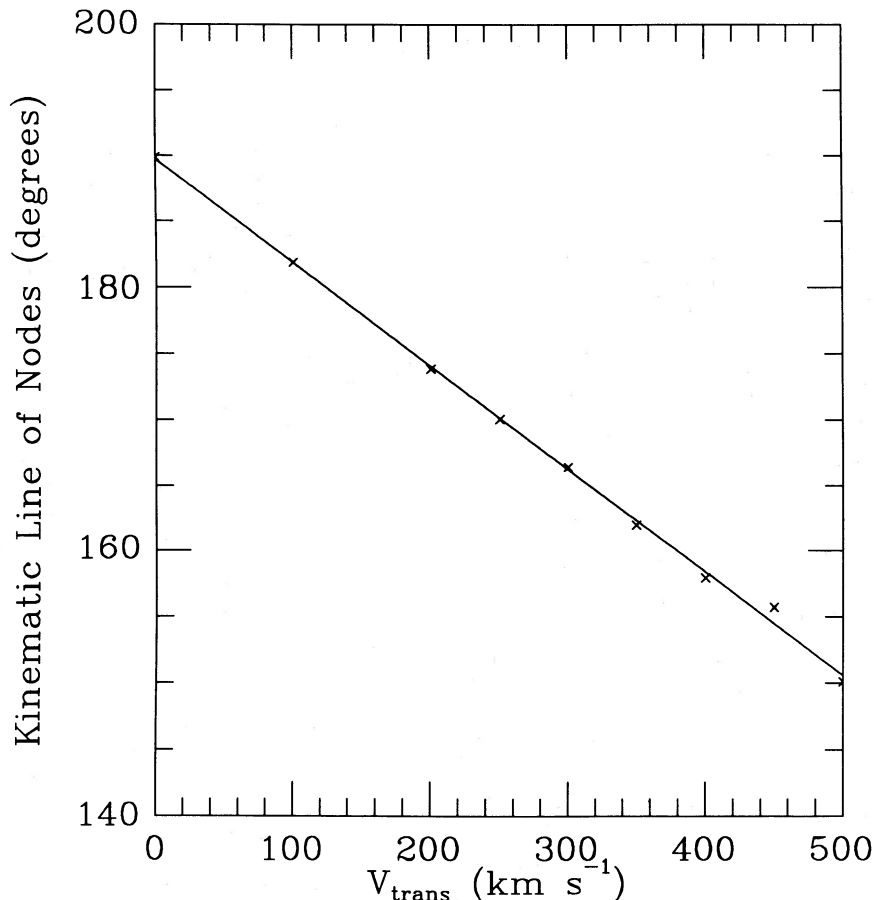


FIG. 2.—Graph showing the effect of varying the transverse velocity (V_{trans}) on the mean position angle of the kinematic line of nodes

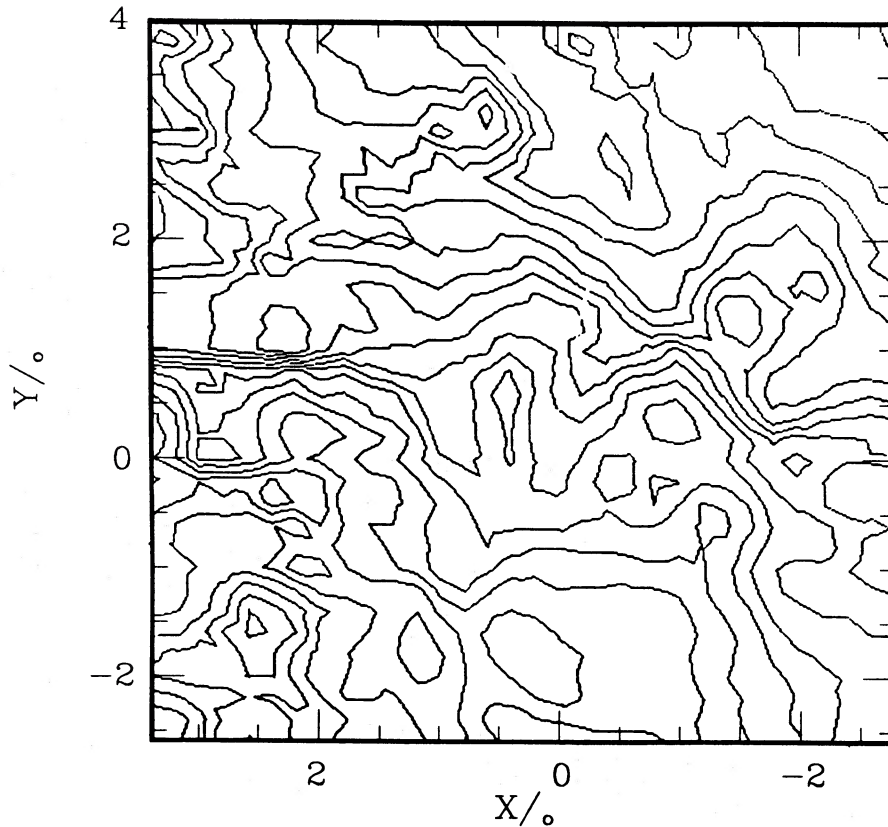


FIG. 3.—Smoothed H I velocity contour map after subtracting the radial velocity component due to a transverse velocity of 275 km s^{-1} . The coordinate system is that due to Isserstedt (1975).

that the LMC—Galactic center distance is always very similar to the adopted LMC—solar distance, and the errors are determined principally by the errors in this distance.

The radial velocity (LSR) of the LMC is $250 \pm 5 \text{ km s}^{-1}$. We adopt $220 \pm 7 \text{ km s}^{-1}$ as the orbital motion of the Sun about the Galactic center (Einasto, Hvald, and J  veer 1979). This geometry can now be used with the transverse velocity of the LMC as seen at the Sun of $275 \pm 65 \text{ km s}^{-1}$, derived above, to derive the radial velocity of the LMC as seen from the Galactic center. This turns out to be very small, only $42 \pm 10 \text{ km s}^{-1}$. We may therefore conclude that the LMC is very close to its perigalacticon, and that its space velocity with respect to the Galactic center is about 278 km s^{-1} . This agrees excellently with the value of 280 km s^{-1} for a perigalactic distance of 52 kpc claimed by Mathewson (1976) using a different approach to ours.

The fact that the LMC is near its perigalacticon allows us to put an *indicative* upper limit on the mass of the Galaxy out to 51 kpc, by assuming that the LMC has fallen from rest from infinity to its current distance. This gives $M_{\text{gal}} = 4.5 \times 10^{11} M_{\odot}$. This is in good agreement with White and Frenk (1983), who obtained $5 \times 10^{11} M_{\odot}$ out to 33 kpc, using systems in the outer halo of our Galaxy. The derived mass of the Galaxy would double if the Magellanic Clouds are in fact in a circular orbit and could be reduced by an arbitrary factor if the LMC is in a hyperbolic orbit.

d) The Mass and Rotation Curve of the LMC

The rotation curve, obtained from a strip of $\pm 15^{\circ}$ in position angle passing through the centroid of the PN distribution

(Sanduleak 1984) and deprojected for an inclination of 33° (Feitzinger, Isserstedt, and Schmidt-Kaler 1977), is shown in Figure 4. Note that this curve is approximately symmetric about $r = +0.5$ and not about the PN centroid. Note also that the central ± 1.5 is strongly perturbed, possibly as a result of the gas streaming motions expected as a result of an asymmetric positioning of the bar (de Vaucouleurs and Freeman 1973; Feitzinger 1983). Folding this curve about its point of symmetry, which we adopt as the rotation center, gives the average rotation curve as shown in Figure 5.

The rotation curve does not fit well to a Keplerian curve, even in the outer regions. Usually, an exponential disk is taken as giving acceptable fit to the rotation curve of Magellanic type galaxies (Freeman 1970). The mass is then given in terms of the maximum rotation velocity, V_{max} , by

$$V_{\text{max}} = 0.623(GM_{\text{exp}}\alpha)^{1/2}, \quad (1)$$

where α , the photometric scale length is taken as 0.010 per arcmin, corresponding to a disk scale length of 1.6 kpc (de Vaucouleurs 1960). This gives $M_{\text{exp}} = (3.2 \pm 0.3) \times 10^9 M_{\odot}$, where the uncertainty in the distance of the LMC has been taken into account. However, a better fit to the rotation curve would be obtained assuming solid-body rotation out to 2.0° from the center of symmetry, with an exponential disk outside that. Fitting this disk model gives our best estimate of the mass of the LMC out to 3° ; $(4.6 \pm 0.2) \times 10^9 M_{\odot}$. If the exponential disk continues out to 6° , which is about the largest acceptable value from H I observations (Mathewson and Ford 1984) or from photometry (de Vaucouleurs 1957), then a total mass of $(6.0 \pm 0.6) \times 10^9 M_{\odot}$ is estimated. These figures are entirely

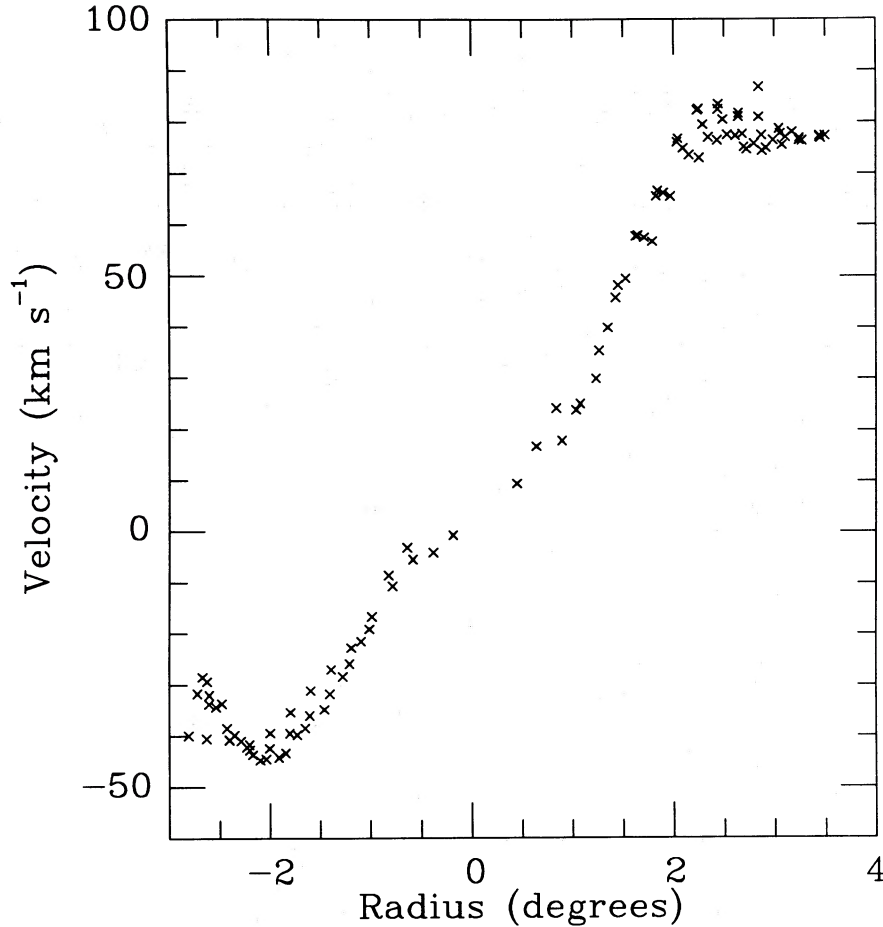


FIG. 4.—LMC rotation curve derived from the H I survey, corrected for a transverse velocity of 275 km s^{-1} , obtained by taking a sector $\pm 15^\circ$ wide along the photometric line of nodes.

consistent with the estimate of $(5 \pm 1) \times 10^9 M_\odot$ for the total mass of the LMC estimated from a variety of mass models by Feitzinger (1979).

e) Rotation Solutions for the H I and Planetary Nebulae

The PN in the SMC present strong evidence for a considerable tidal disruption of this system (Dopita *et al.* 1985). Freeman, Illingworth, and Oemler (1983) presented evidence from clusters to suggest that the same might well be true for the LMC. It is therefore of great interest to compare the PN and H I dynamics to search for such effects. The simplest exercise that can be done is to simply compare the radial velocity of each PN with the H I in its vicinity. This has been done in Figure 6, which should be compared with Figure 4 in Freeman, Illingworth, and Oemler (1983). The diagram shows a poor local correlation between the H I and PN dynamics. However, there is no evidence for the systematic offset in velocity claimed for the older population by Freeman, Illingworth, and Oemler (1983).

Having obtained the form of the rotation curve, a more sophisticated means to analyze the velocity data is derived from that given by Freeman, Illingworth, and Oemler (1983). The rotation solution is given by

$$V(\theta, r) = V_m(r) \{1 \pm [\tan(\theta - \theta_0) \sec i]^2\}^{-0.5} + V_0, \quad (2)$$

$$0 \leq \theta \leq 2\pi,$$

where $V(\theta, r)$ is the rotational velocity projected onto the line of sight at position angle θ and radial coordinate r . We minimized the residuals in this equation using a nonlinear χ^2 -minimization routine from the software package MINUIT. The two free parameters to be minimized with respect to the velocity residuals are θ_0 , the position angle of the line of kinematic line nodes for the whole of the LMC (as opposed to the central region, used in the estimation of the transverse velocity) and V_0 , the systematic Galactocentric velocity of the LMC. We have adopted $V_m(r)$ as the measured H I rotation curve.

Our analysis gave $\theta_0 = 166^\circ$ and $V_0 = 46 \text{ km s}^{-1}$ for the H I solution, and $\theta_0 = 170^\circ$ and $V_0 = 42 \text{ km s}^{-1}$ for the PN population. These figures are identical to within the errors for the two populations. In Figure 7 we show, as a function of azimuthal angle, the velocity difference between the PN radial velocities, and the local H I radial velocities as compared with the rotation solution for the H I. Clearly, the velocity dispersion in the PN population is considerably higher than that of the H I. Notice also that the typical line-of-sight velocity dispersion in the H I is 10 km s^{-1} , but that there are clearly distinct local regions of increased velocity dispersion. These correspond closely in position to supergiant shells of star-forming activity, principally the 30 Dor complex ($\theta = 100^\circ$), the N206 region ($\theta = 240^\circ$), and the region around N186 ($\theta = 320^\circ$). This is further observational proof that star formation has the effect of stirring up the gas in the plane and

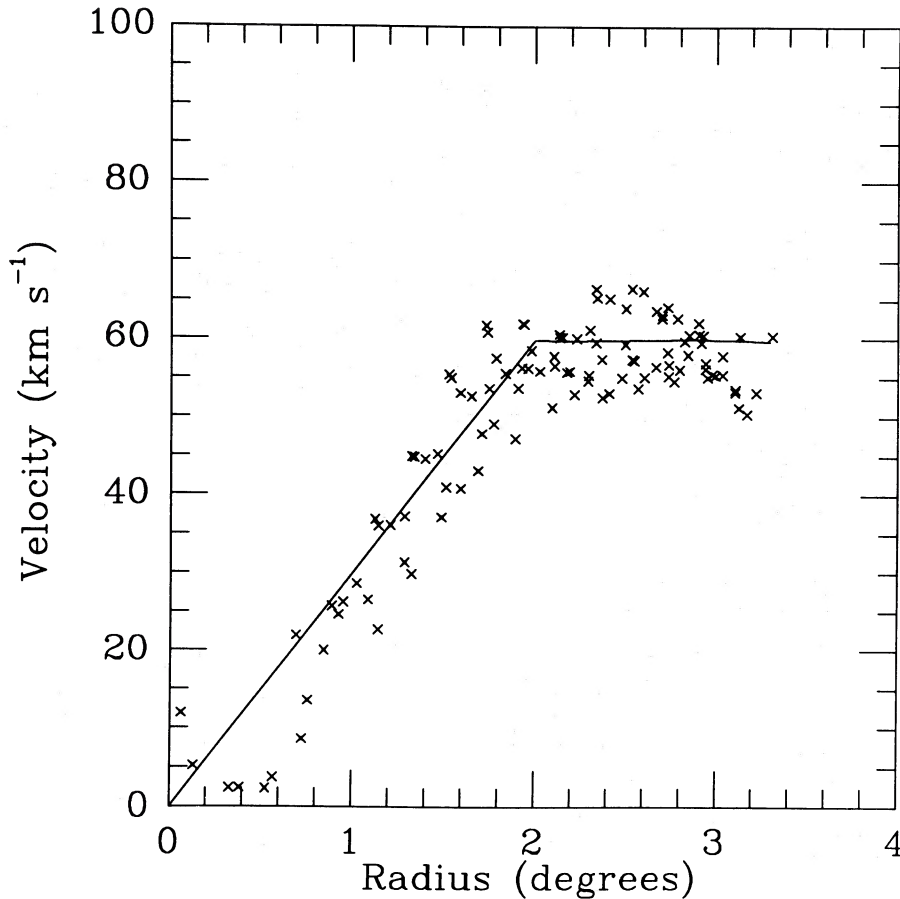


FIG. 5.—LMC rotation curve obtained after folding the H I data about the symmetrical point. The solid line represents the fitted theoretical curve comprising solid body rotation within the inner 2° together with an exponential disk outside that radius.

increasing the vertical velocity dispersion (Dopita, Mathewson, and Ford 1985). By contrast, the PN velocity dispersion is constant and featureless with position angle.

It is possible that the PN population might in fact be a halo population with a lower orbital velocity. To check this possibility, we divided the planetaries into two groups, those with projected radius from the center less than 2° , and the rest. If the PN rotate more slowly than the H I, this would show as a systematic modulation of the velocity residuals with position angle for the outer group. As shown in Figure 8, no such effect is found, implying that the PN population rotates just as fast as the H I.

We can therefore conclude that *there is no significant difference between the H I and the PN kinematics other than an increase in velocity dispersion in the older PN population.* This result confirms and amplifies that foreshadowed by Freeman, Illingworth, and Oemler (1983) and poses an interesting conundrum. If, as claimed by Freeman, Illingworth, and Oemler (1983), the old clusters have a rotation axis that differs from the young solution by $\sim 50^\circ$, how then could this have occurred? As pointed out in that paper, such a tilt is not stable and can persist only for a time scale of order 10^9 yr, unless the older clusters define the form of the gravitational potential of the LMC, a hypothesis for which there is little supporting evidence. The most profound dynamical disturbance that may have been experienced by the LMC would have been a near collision with the SMC that may have occurred $\sim 2 \times 10^8$ yr

ago (Murai and Fujimoto 1980), resulting in profound tidal disturbance to the SMC (Mathewson and Ford 1984; Dopita *et al.* 1985; Mathewson, Ford, and Visvanathan 1986). We can therefore conclude *either* that the PN population is younger than 2×10^8 yr old *or* that this collision did not result in the twisting of the rotation axes implied by the old clusters.

f) *Orbital Diffusion and the Age of the Planetary Nebulae*

We demonstrated in the previous section that there is no evidence that the PN represent a halo population. However, the PN population undeniably does have a much larger velocity dispersion than the H I. An increase in velocity dispersion is a natural consequence of a greater age. The process was examined by Spitzer and Schwarzschild (1951, 1953) who showed that orbital diffusion can occur as a consequence of "gravitational Fermi scattering," the encounter between stars and giant molecular clouds (GMCs). The relaxation time (10^8 yr) for such encounters is much shorter than for star-star encounters (10^{14} yr) as a consequence of the large characteristic mass of the GMCs, typically of order $10^5 M_\odot$. The relationship between total velocity dispersion at time t , $V(t)$, and the initial velocity dispersion, $V(0)$, of a stellar population is given by

$$V(t) = V(0)[1 + t/t_e]^{1/3}, \quad (3)$$

where the encounter time scale, t_e , is given in terms of the number of clouds per unit volume, n_c , their average mass, m_c ,

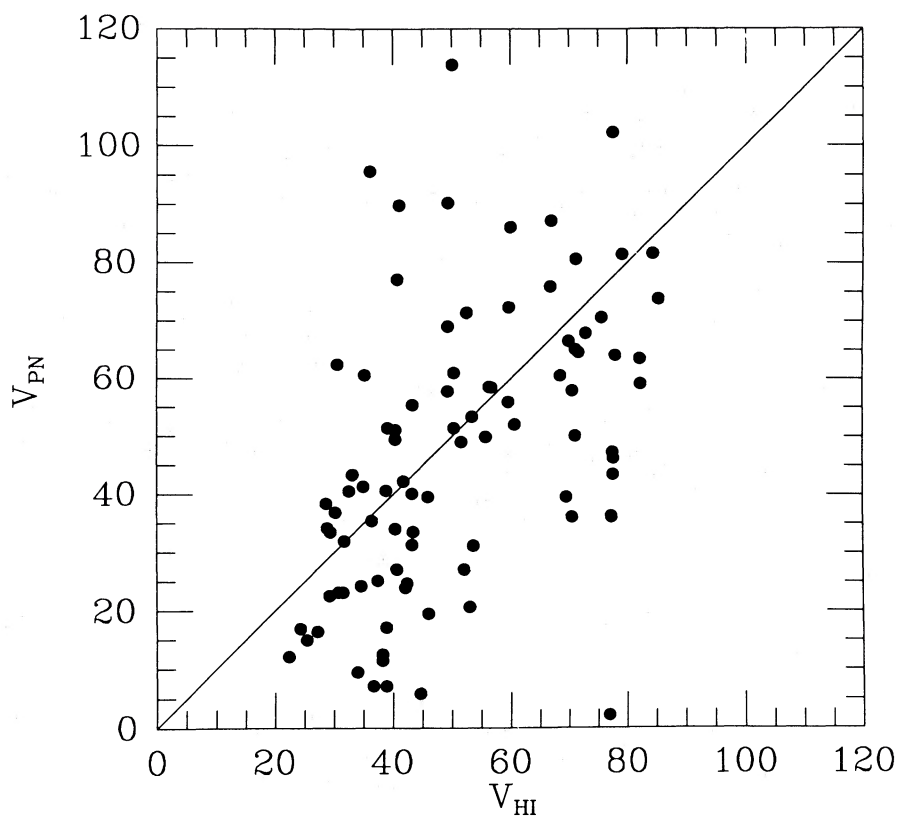


FIG. 6.—The observed GSR velocity for each planetary nebula in km s^{-1} compared to the H I velocity at each PN's position. Equality is indicated by the line of slope unity. The error in the velocity measurement is no larger than the size of each symbol.

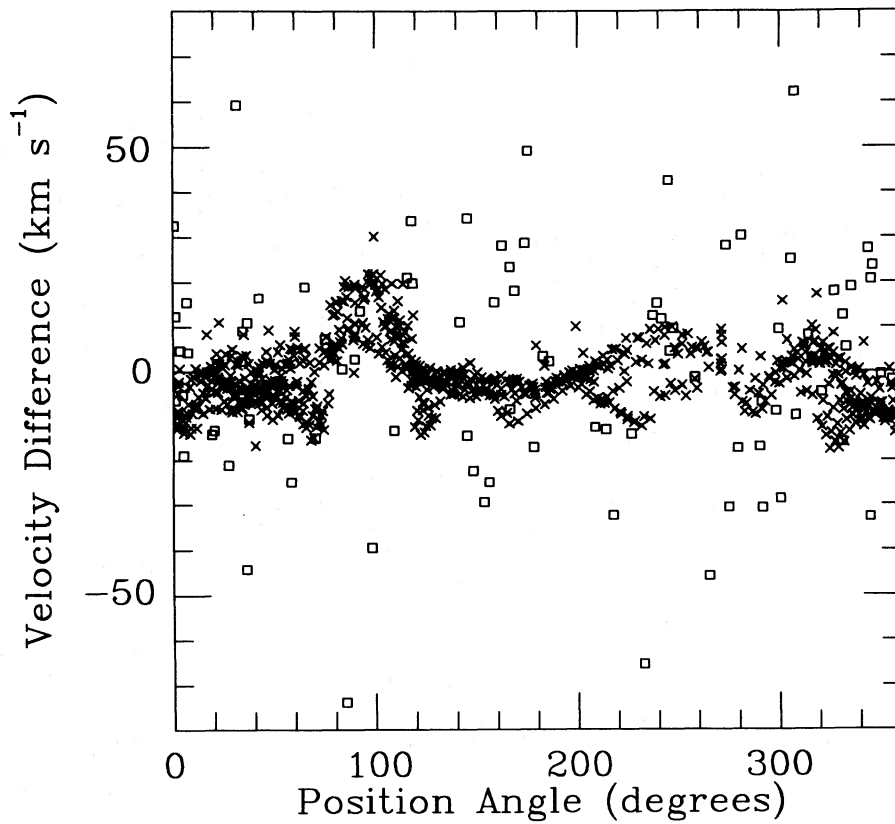


FIG. 7.—The velocity difference obtained from the H I data (*crosses*) and the planetary nebulae (*squares*). The 30 Doradus complex is clearly visible at position angle 100° , as are other star-forming regions near 240° and 320° .

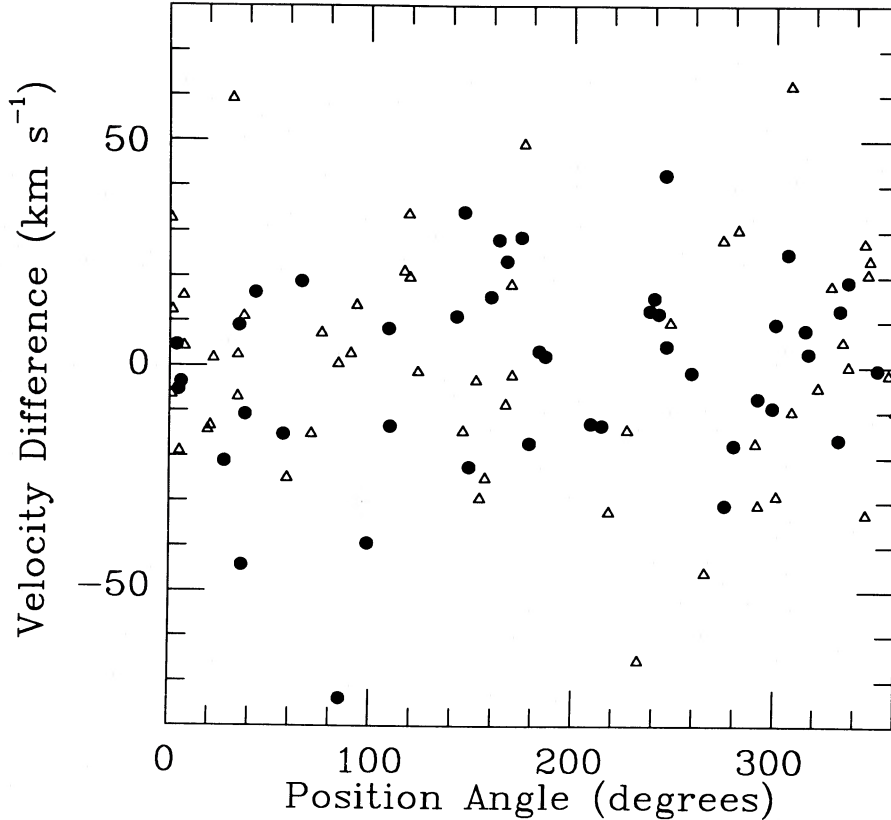


FIG. 8.—The velocity difference as a function of position angle for the planetary nebulae when they are split into two groups. Those inside $r = 2^\circ$ (filled circles) and those outside that radius (triangles).

and an impact parameter function a (~ 9.8) by

$$t_e = 4V_m^3(0)/[3\pi^{3/2}G^2n_c m_c^2 \ln(a)]. \quad (4)$$

The accuracy of such a formula is determined both by the evolution of the disk GMC population, and by the reduction of interaction events when the orbits have diffused sufficiently to take them out of the region of the disk occupied by the GMCs for a significant portion of the orbit. Both of these tend to reduce the rate of the diffusion with time. Wielen (1977) examined the diffusion rate by direct observation of populations of various ages in the solar neighborhood. He found that an equation of similar form to equation (3) gives an adequate description, but with an exponent of $\frac{1}{2}$ and an encounter time scale of 5×10^7 yr. Subsequent theoretical studies (Vader and de Jong 1981; Villumsen 1985) have tended to confirm the lower value for the exponent.

As dynamical evolution proceeds, the velocity ellipsoid does not remain spherical, because radial diffusion is more active than axial diffusion. Wielen finds that, for a dynamically old population, the ratio of axial to radial velocity dispersions, $\sigma_w : \sigma_r$, tends to 0.6:1.0. With this fact, we can transform the observed line-of-sight velocity differences to a histogram of the vertical (or axial) velocity dispersion in the LMC, assuming that the PN population is dynamically old, and that the H I is dynamically young. These are shown in Figures 9 and 10, from which we conclude that $\sigma_w(\text{H I}) = 5.4 \text{ km s}^{-1}$ and $\sigma_w(\text{PN}) = 19.1 \text{ km s}^{-1}$ (FWHM). These figures imply a total velocity dispersion of $\sigma_T(\text{H I}) = 9.4 \text{ km s}^{-1}$ and $\sigma_T(\text{PN}) = 37.1 \text{ km s}^{-1}$, using the ratios of vertical to axial velocity dispersion given above. The vertical velocity dispersion of the H I is very similar

to the values of $7\text{--}10 \text{ km s}^{-1}$ found by van der Kruit and Shostak (1984 and references therein) in other disk galaxies covering a wide variety of morphological types. The velocity dispersion in these galaxies does not appear to depend on radial coordinate or vary much between arm and interarm regions and can be understood as a consequence of self-regulating feedback in star-formation activity (Dopita 1986).

Are the observations consistent with the hypothesis that the increase in velocity dispersion is the result of the operation of the stellar orbital diffusion process described above? The answer to this question requires a knowledge of the age distribution of the precursor stars. Fortunately, the precursor mass of the stars giving rise to the PN can be estimated fairly accurately from existing observational and theoretical material. The mass distribution for LMC stars leaving the asymptotic giant branch (AGB) has been computed by Weidemann (1987), using the luminosity function derived for these stars by Reid and Mould (1984). This is a very sharply peaked function with a maximum at $0.59 M_\odot$, and which is skewed to higher masses, with 80% of stars lying below $0.70 M_\odot$. The relationship between this mass and the initial mass depends on the mass-loss rate in the AGB phase of evolution and has been determined for these same stars by Wood, Bessell, and Fox (1983). From this work, we can conclude that most of the LMC planetaries had initial stellar masses near $0.88 M_\odot$, but there exists a tail in the distribution extending to about $1.4\text{--}1.6 M_\odot$. This is in good agreement with the figure obtained by simply adding the typical mass of the central star ($0.6 M_\odot$) to the largest ionized mass measured for optically thin nebulae ($0.5 M_\odot$; Wood *et al.* 1987).

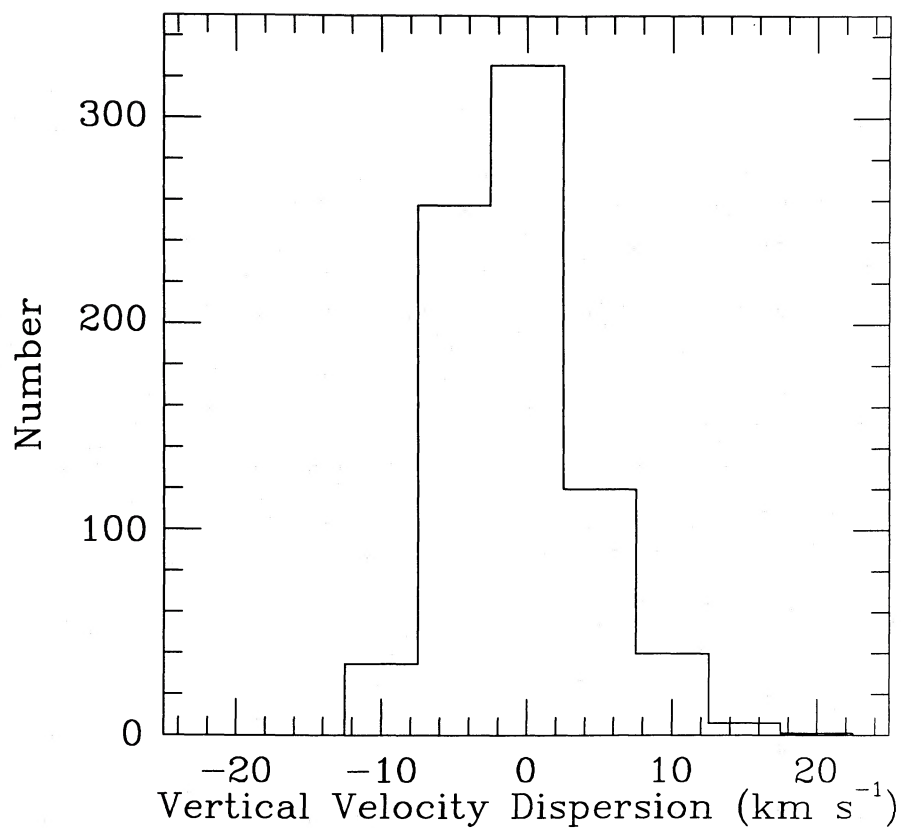


FIG. 9.—Histogram of the derived vertical velocity dispersion (σ_w) for the H I data. The tail extending to +20 km s^{-1} is due to the 30 Doradus region. The full width at half-maximum is 6 km s^{-1} .

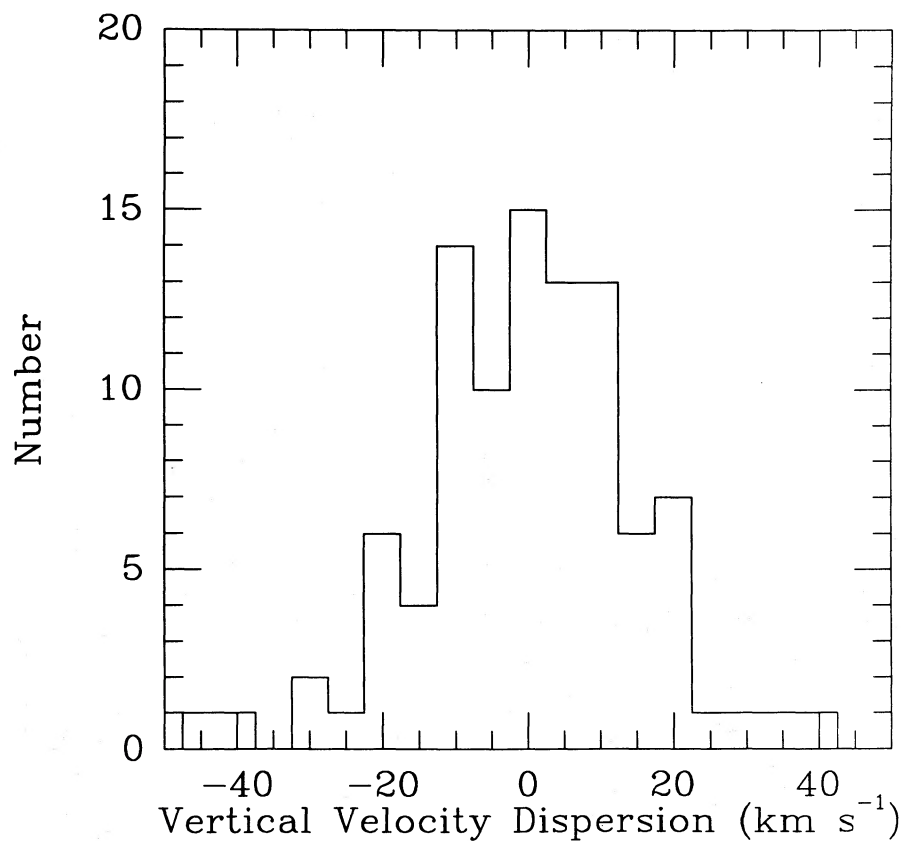


FIG. 10.—Histogram of the derived vertical velocity dispersion (σ_w) for the planetary nebulae. The full width at half-maximum is 19 km s^{-1} .

The typical ages of these stars at the time of PN formation can be estimated from the main-sequence lifetimes given by Iben and Tutukov (1985), assuming that this occupies 90% of the total lifetime of the planetary nebula precursor star. This shows that the bulk of the PN have an age of near 3.5×10^9 yr, but there are also younger objects present down to an age of order $(0.5\text{--}1.3) \times 10^9$ yr. Thus, the PN population predates, by a considerable margin, any encounter between the LMC and SMC but is insufficiently aged to have been formed during the initial collapse of the LMC.

These ages can now be substituted in either the Wielen (1977) diffusion coefficients or the Spitzer and Schwarzschild (1951, 1953) formulae, equations (3) and (4) above. The principal uncertainty in the use of these equations is the mass appropriate for the giant H I clouds in the LMC. The H I data do not have sufficient resolution to see these, and although these are seen in the CO data (Cohen, Montani, and Rubio 1984), the low abundance of both C and O renders a mass calculation uncertain. Using a mass density of 3×10^{-24} g cm $^{-3}$ in equations (3) and (4), the PN age derived above, and the observed velocity dispersions of the H I and PN population implies that the mass of the typical scattering cloud is $\sim 1.6 \times 10^5 M_{\odot}$. This should be compared with the value found for Galactic molecular clouds, $1.5 \times 10^5 M_{\odot}$ (Liszt, Delin, and Burton 1981). Thus, diffusive processes appear to work in the same way, and on the same timescale in the LMC as in the local region of our Galaxy.

This conclusion can be checked using Wielen's work. With the observed velocity dispersions, and using a constant diffusion coefficient of 6.0×10^{-7} (km s $^{-1}$) yr $^{-1}$, the indicative age of the PN population is 2.1×10^9 yr. Using his velocity-dependent diffusion formulae give ages of $(2.5\text{--}3.6) \times 10^9$ yr. Both of these figures are sufficiently close to the ages given above to give us confidence that diffusive processes are very similar to those operating in our local region of the Galaxy.

IV. CONCLUSIONS

From radial velocity data for a very extensive sample of planetary nebulae in the LMC, we have established that the

PN population forms a flattened disk with almost the same spatial distribution and rotation solution as the H I layer. The vertical velocity dispersion of the PN is consistent with the action of orbital diffusion over the lifetime typical for the PN precursor stars. While there may be a few objects in the sample sufficiently old to be considered halo objects, it is clear that the bulk of the PN cannot represent a halo population.

This result must be reconciled with the Freeman, Illingworth, and Oemler (1983) finding that the rotation axis of old ($> 1\text{--}2 \times 10^9$ yr) clusters have a rotation axis twisted by some 50° with respect to the younger. The age of the PN is sufficient that we can exclude the possibility that this twisting has been caused by tidal torques during a recent close encounter of the LMC with the SMC. On the other hand, there is no evidence to support the idea that the old clusters provide the gravitational potential in which the H I and younger stellar components move. The question of the reality and cause of the twisting of the cluster population remains open.

From a reanalysis of the H I data, we have also been able to derive a figure for the transverse velocity of the LMC, assuming that the LMC is moving along the small circle defined by the Magellanic stream and that the kinematic and photometric line of nodes agree. This gave a transverse velocity of 275 ± 65 km s $^{-1}$, which implies that the LMC is near perigalacticon. An indicative mass of the Galaxy out to 51 kpc is therefore $4.5 \times 10^{11} M_{\odot}$, derived on the assumption that the LMC has fallen to its current position from rest at infinity. Finally, from our new rotation curve, we estimate the mass of the LMC to be $(4.5 \pm 0.3) \times 10^9 M_{\odot}$ out to $r = 3^\circ$; and of order $6 \times 10^9 M_{\odot}$ in total.

H. C. F. wishes to thank the Australian National University for a visiting fellowship held during the early part of the work described in this paper, and M. A. D. wishes to thank the Space Telescope Science Institute for hospitality and support under their Visiting Scientist program, during which this work advanced.

REFERENCES

- Bevington, P. R. 1969, *Data Reduction and Error Analysis in the Physical Sciences* (New York: McGraw-Hill).
- Calet, A., Deharveng, L., Georgelin, Y. M., and Georgelin, Y. P. 1982, *Astr. Ap.*, **110**, 185.
- Cohen, R., Montani, J., and Rubio, M. 1984, in *IAU Symposium 108, Structure and Evolution of the Magellanic Clouds*, ed. S. van den Bergh and K. S. de Boer (Dordrecht: Reidel), p. 401.
- de Vaucouleurs, G. 1957, *A.J.*, **62**, 69.
- . 1960, *Ap. J.*, **131**, 574.
- de Vaucouleurs, G., and Freeman, K. C. 1973, *Vistas Astr.*, **14**, 163.
- Dopita, M. A. 1987, in *Nearly Normal Galaxies from the Planck Time to the Present*, ed. S. M. Faber (Berlin: Springer), in press.
- Dopita, M. A., Ford, H. C., Lawrence, C. J., and Webster, B. L. 1985, *Ap. J.*, **296**, 390.
- Dopita, M. A., Ford, H. C., and Webster, B. L. 1985, *Ap. J.*, **297**, 593.
- Dopita, M. A., Mathewson, D. S., and Ford, V. L. 1985, *Ap. J.*, **297**, 599.
- Dopita, M. A., Meatheringham, S. J., Webster, B. L., and Ford, H. C. 1988, *Ap. J.*, **327**, 639.
- Dopita, M. A., Meatheringham, S. J., Wood, P. R., Webster, B. L., Morgan, D. H., and Ford, H. C. 1987, *Ap. J. (Letters)*, **315**, L107.
- Einasto, J., Hval, U., and Jöeveer, M. 1979, in *The Large Scale Structure of the Galaxy*, ed. W. D. Burton (Dordrecht: Reidel), p. 231.
- Feast, M. W. 1968, *M.N.R.A.S.*, **140**, 345.
- . 1984, *So. African Obs. Circ.*, No. 397.
- Feitzinger, J. V. 1979, Ph.D. thesis, Astronomisches Institut der Ruhr-Universität, Bochum.
- Feitzinger, J. V. 1980, *Space Sci. Rev.*, **27**, 35.
- . 1983, in *IAU Symposium 100, Internal Kinematics and Dynamics of Galaxies*, ed. E. Athanassoula (Dordrecht: Reidel), p. 214.
- Feitzinger, J. V., Isserstedt, J., and Schmidt-Kaler, Th. 1977, *Astr. Ap.*, **57**, 265.
- Freeman, K. C. 1970, *Ap. J.*, **160**, 811.
- Freeman, K. C., Illingworth, G., and Oemler, A. 1983, *Ap. J.*, **272**, 488.
- Fujimoto, M., and Murai, T. 1984, in *The Structure and Evolution of the Magellanic Clouds*, ed. S. van den Bergh and K. S. de Boer (Dordrecht: Reidel), p. 115.
- Graham, J. A. 1979, in *The Large Scale Structure of the Galaxy*, ed. W. D. Burton (Dordrecht: Reidel), p. 195.
- Henize, K. G. 1956, *Ap. J. Suppl.*, **2**, 315.
- Henize, K. G., and Westerlund, B. E. 1963, *Ap. J.*, **137**, 747.
- Iben, I., and Tutukov, A. V. 1985, *Ap. J. Suppl.*, **58**, 661.
- Isserstedt, J. 1975, *Astr. Ap.*, **41**, 21.
- Jacoby, G. H. 1980, *Ap. J. Suppl.*, **42**, 1.
- Lin, D. N. C., and Lynden-Bell, D. 1982, *M.N.R.A.S.*, **198**, 707.
- Lindsay, E. M., and Mullen, D. J. 1963, *Irish A.J.*, **6**, 51.
- Liszt, H. S., Delin, X., and Burton, W. B. 1981, *Ap. J.*, **249**, 532.
- McGee, R. X., and Milton, J. A. 1964, in *IAU Symposium 20, The Galaxy and the Magellanic Clouds*, ed. F. J. Kerr and A. W. Rodgers (Canberra: Australian Acad. Sci.) p. 289.
- . 1966a, *Australian J. Phys.*, **19**, 343.
- . 1966b, *Australian J. Phys. A. Suppl.*, No. 2.
- Mathewson, D. S. 1976, *Royal Greenwich Obs. Bull.*, No. 182.
- . 1984, *Mercury*, **13**, 57.

- Mathewson, D. S., Cleary, M. N., and Murray, J. D. 1974, *Ap. J.*, **190**, 291.
 Mathewson, D. S., and Ford, V. L. 1984, in *IAU Symposium 108, Structure and Evolution of the Magellanic Clouds*, ed. S. van den Bergh and K. S. de Boer (Dordrecht: Reidel), p. 125.
 Mathewson, D. S., Ford, V. L., and Visvanathan, N. 1986, *Ap. J.*, **301**, 664.
 Mathewson, D. S., Schwartz, M. P., and Murray, J. D. 1977, *Ap. J. (Letters)*, **217**, L5.
 Meaburn, J. 1981, in *Investigating the Universe*, ed. F. D. Kahn (Dordrecht: Reidel), p. 61.
 Meatheringham, S. J., Dopita, M. A., and Morgan, D. H. 1988, *Ap. J.*, in press.
 Meurer, G. R., Bicknell, G. V., and Gingold, R. A. 1985, *Proc. Astr. Soc. Australia*, **6**, 195.
 Morgan, D. H. 1984, private communication.
 Morgan, D. H., and Good, A. R. 1985, *M.N.R.A.S.*, **213**, 491.
 Murai, T., and Fujimoto, M. 1980, *Pub. Astr. Soc. Japan*, **32**, 581.
 Reid, N., and Mould, J. 1984, *M.N.R.A.S.*, **284**, 98.
 Rohlf, K., Kreitschmann, J., Siegmann, B. C., and Feitzinger, J. V. 1984, *Astr. Ap.*, **137**, 343 (RKSF).
 Sanduleak, N. 1984, in *IAU Symposium 108, Structure and Evolution of the Magellanic Clouds*, ed. S. van den Bergh and K. S. de Boer (Dordrecht: Reidel), p. 231.
 Sanduleak, N., McConnell, D. J., and Philip, A. G. D. 1978, *Pub. A.S.P.*, **90**, 621.
 Smith, H. C., and Weedman, D. W. 1972, *Ap. J.*, **177**, 595.
 Spitzer, L., and Schwarzschild, M. 1951, *Ap. J.*, **114**, 385.
 ———. 1953, *Ap. J.*, **118**, 106.
 Stapinski, T. E., Rodgers, A. W., and Ellis, M. J. 1981, *Pub. A.S.P.*, **93**, 242.
 Vader, J. P., and de Jong, T. 1981, *Astr. Ap.*, **100**, 124.
 van der Kruit, J. P., and Shostak, G. S. 1984, *Astr. Ap.*, **134**, 258.
 Villumsen, J. V. 1985, *Ap. J.*, **290**, 75.
 Visvanathan, N. 1985, *Ap. J.*, **288**, 182.
 Webster, B. L. 1969, *M.N.R.A.S.*, **143**, 79.
 Weidemann, V. 1987, in *Late Stages of Stellar Evolution*, ed. S. Kwok and S. R. Pottasch (Dordrecht: Reidel), p. 347.
 White, S. D., and Frenk, C. S. 1983, in *Kinematics, Dynamics, and Structure of the Milky Way*, ed. W. L. Shuter (Dordrecht: Reidel), p. 343.
 Wielen, R. 1977, *Astr. Ap.*, **60**, 263.
 Wood, P. R., Bessell, M. S., and Dopita, M. A. 1986, *Ap. J.*, **311**, 632.
 Wood, P. R., Bessell, M. S., and Fox, M. W. 1983, *Ap. J.*, **272**, 99.
 Wood, P. R., Dopita, M. A., and Bessell, M. S. 1985, *Proc. Astr. Soc. Australia*, **6**, 54.
 Wood, P. R., Meatheringham, S. J., Dopita, M. A., and Morgan, D. H. 1987, *Ap. J.*, **320**, 178.

MICHAEL A. DOPITA and STEPHEN J. MEATHERINGHAM: Mt. Stromlo and Siding Spring Observatories, Australian National University, Private Bag, Woden P.O., ACT 2606, Australia

HOLLAND C. FORD: Space Telescope Science Institute, Homewood Campus, Baltimore, MD 21218

B. LOUISE WEBSTER: School of Physics, University of New South Wales, P.O. Box 1, Kensington, NSW 2033, Australia